Extracting Temperature and Emissivity from High Spatial Resolution Multispectral Thermal Infrared Data

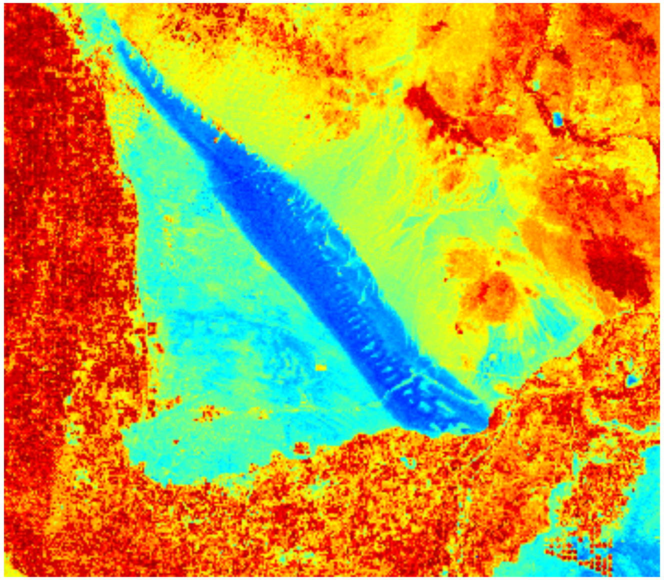

Simon Hook, Glynn Hulley

Jet Propulsion Laboratory, California Institute of Technology, Pasadena, CA

Outline

- Introduction
- Thermal Infrared Remote Sensing
- Atmospheric Correction
- Temperature Emissivity Separation
- ASTER-GEM
- MODIS LST&E (MOD21)
- Validation

Introduction

- **Land Surface Emissivity:** ratio between actual emitted radiation, and radiation emitted by a blackbody at the same temperature (typically varies from 0.6 – 0.99)

$$\epsilon_\lambda = \frac{L_\lambda}{L_\lambda(BB)}$$

- **Land Surface Temperature (LST):** how 'hot' the skin surface of the Earth feels at any given time

- LST and emissivity closely coupled variables, both determine amount of thermal radiation emitted by the Earth's surface, BUT are independent measurements!
  - Emissivity is intrinsic property of the Earth's surface
  - LST varies with local atmospheric conditions and irradiance history
  - Emissivity error of 0.015 = ~1 K LST error

Motivation:

Why is Land Surface Temperature/Emissivity (LST&E) Important?

- Climate and Hydrological Modeling
  - LST is a critical component for evapotranspiration modeling (e.g. ALEXI)
  - Emissivity set to constant value (eg. 0.96) with simple parameterizations in land models, e.g. NCAR Community Land Model (CLM3)
  - Simulations by Zhou et al. (2003) showed emissivity decrease of 0.1 resulted in 7 W/m^2 underestimation longwave radiation estimates (greenhouse gases, ~2 W/m^2)
- Atmospheric Retrievals
  - Boundary layer temperature and water vapor over land are heavily dependent on accurate LST&E, eg. Emissivity error of 0.15 leads to more than 3 K error in temperature retrievals in boundary layer (Kornfield and Susskind, 1977)
- Land use, Land cover change (LCLUC)
  - Increased demand for agricultural land, and significant land cover changes from extreme climatic events => increased demand for LST&E products for monitoring these events
- Soil Moisture Mapping
  - Evapotranspiration models require LST&E to characterize surface energy balance
  - LST will be critical input for NASA's future Soil Moisture Active & Passive (SMAP) mission

NASA LST&E Product Characteristics

	ASTER (Advanced Spaceborne Thermal Emission and Reflection Radiometer)	HyspIRI (Hyperspectral Infrared Imager)	MODIS (Moderate Resolution Imaging Spectroradiometer)	AIRS (Atmospheric Infrared Sounder)
Satellite	Terra (2000)	Expected launch: 2020+	Terra/Aqua (2000/2002)	Aqua (2002)
Calibration	<0.3 K	<0.2 K	<0.2 K	<0.2 K
LST&E Algorithm	TES Calibration Curve	TES Calibration Curve	1. Day-Night 2. Split-Window	Regression plus simultaneous retrieval
LST&E Product	AST05/08	tbd	MOD11A1/B1/C3	AIRSX2RET
ATBD LST Product Accuracy	1K	1K	1K	2-3 K
Product versions	Version 3	n/a	C4.1, 4.0 and 5.0	Version 4 and 5
Temporal sampling	16 day repeat (1030 AM/PM)	5 day repeat (1030 AM/PM)	Twice-daily (10:30/1:30 AM/PM)	Twice-daily (10:30 AM/PM)
Spatial resolution	90 m	60 m	5 km (c4), 6 km (c5)	45 km
Spectral resolution	5 TIR bands (8-12 µm)	8 TIR bands (4-12 µm)	7 MIR/TIR bands (3.7-14 µm)	39 'hinge-points' (3.7-15.4 µm)
Swath Width	60 km	600 km	2330 km	1650 km

Sensor Spatial Resolution Differences

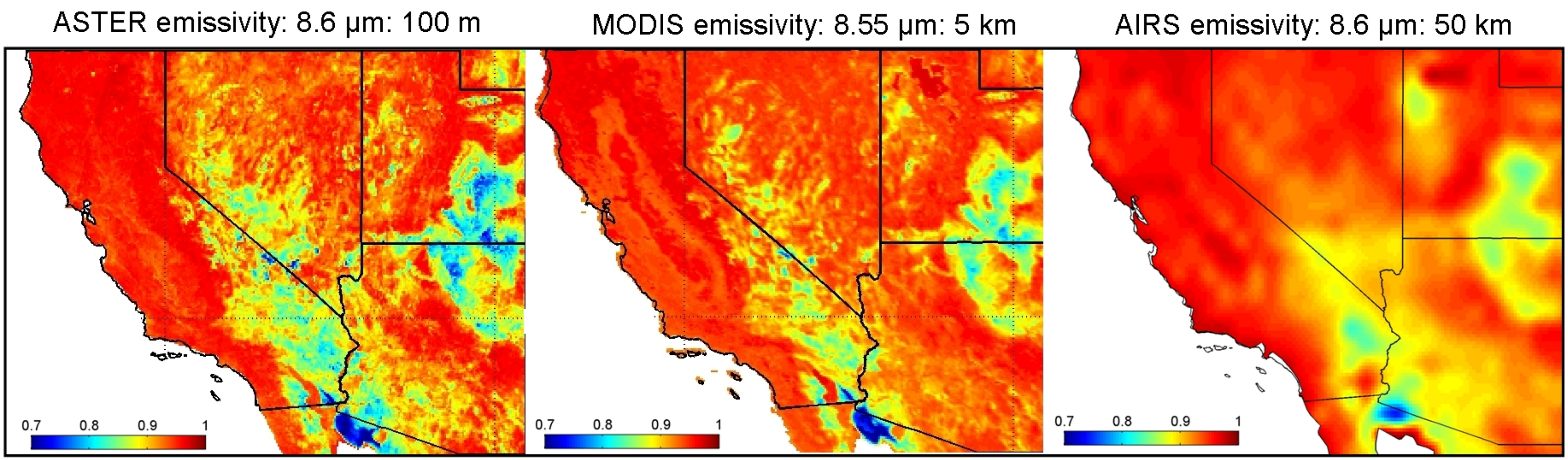

At spatial resolutions < 100m capture variation at the field scale

Thermal Infrared Radiative Transfer

TOA Radiance

$$L_i(\theta) = \overbrace{\underbrace{\tau_i(\theta)\cdot e_i \cdot B_i(T_S)}_{\text{Surface Emission}} + \underbrace{\tau_i(\theta)\cdot(1-e_i)\cdot \overline{L}_i^{\downarrow}}_{\text{Surface Reflection}}}^{\text{Surface Radiance}} + \underbrace{\int B_i(T(P))\,d\tau_i}_{\text{Atmospheric Emission}}$$

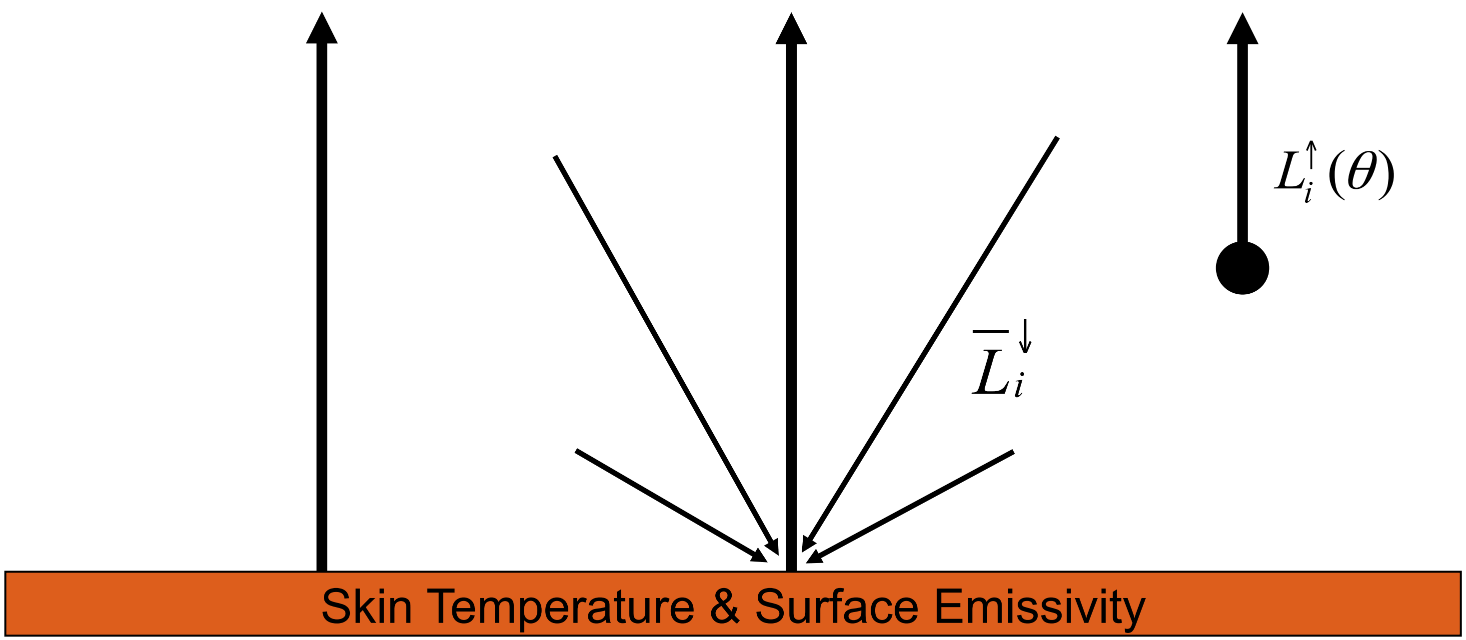

HyspIRI Response Functions

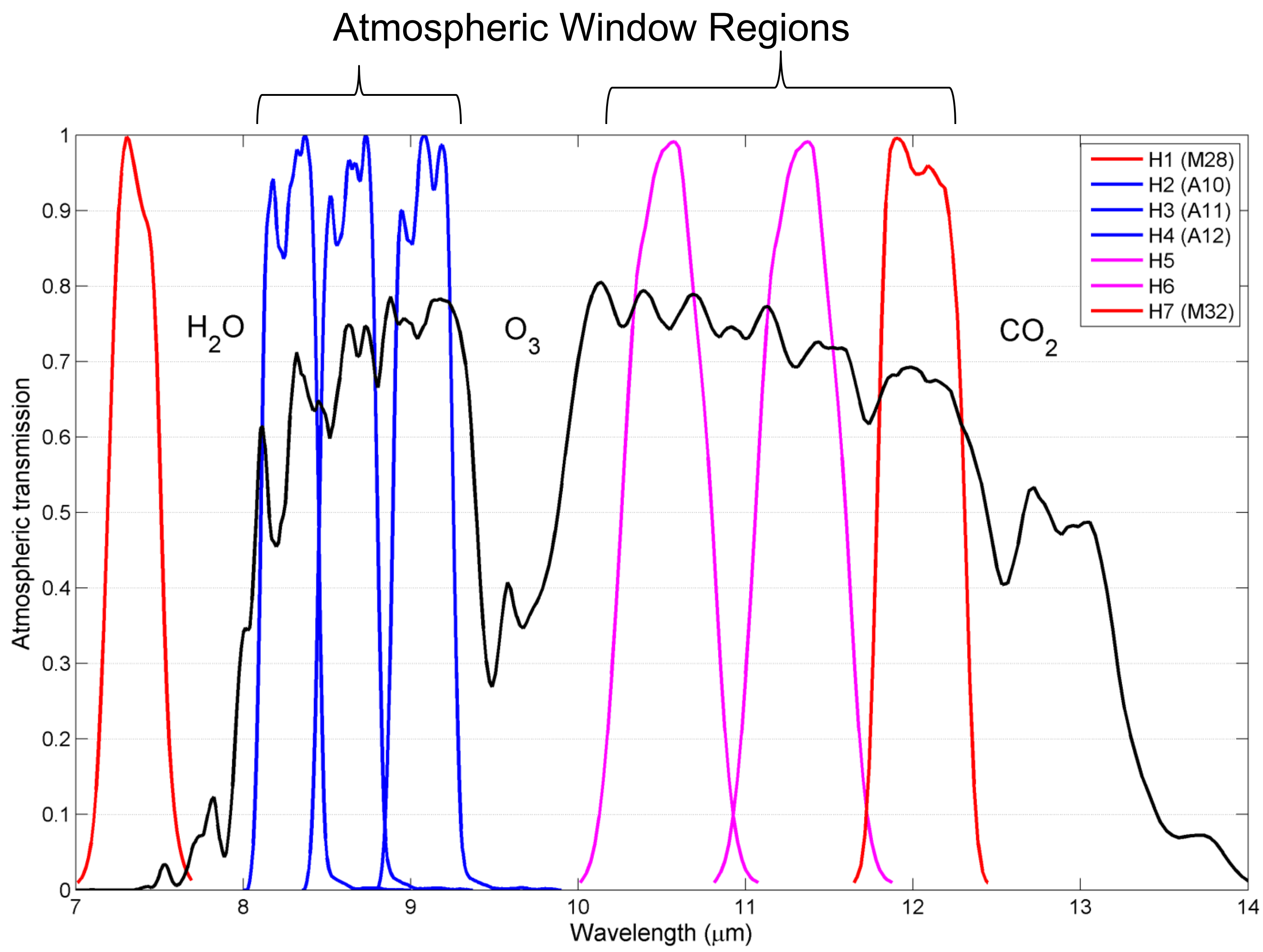

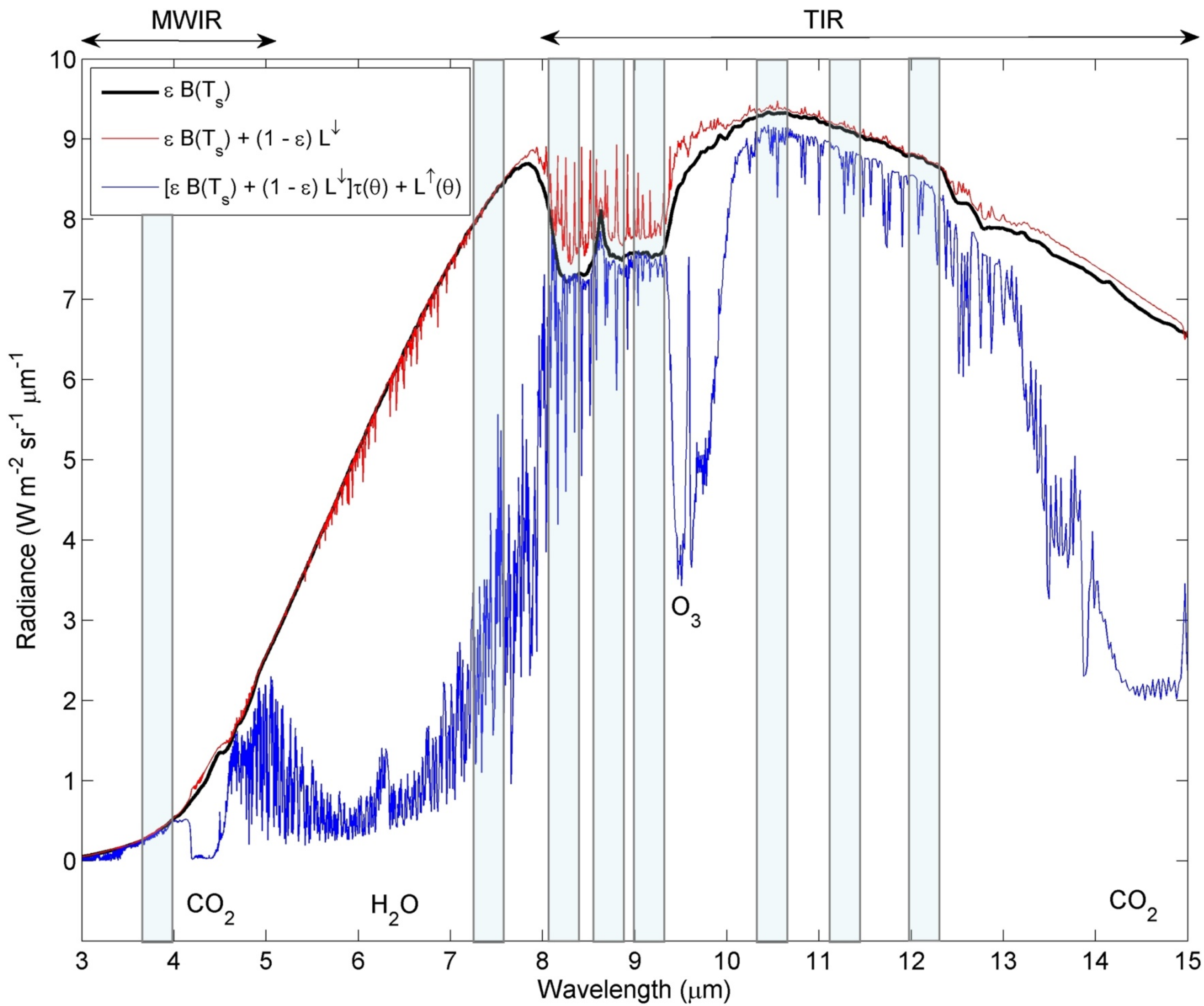

MWIR
TIR
ε B(T_s)
ε B(T_s) + (1 - ε) L↓
[ε B(T_s) + (1 - ε) L↓]τ(θ) + L↑(θ)
Radiance (W m^-2 sr^-1 μm^-1)
Wavelength (μm)
CO2
H2O
O3
CO2

Atmospheric Correction

Observed Radiance

Surface Radiance:

$$L_{surf,i} = e_i \cdot B_i(T_S) + (1-e_i) \cdot \boxed{\overline{L}_i^{\downarrow}} = \frac{L_i(\theta) - \boxed{L_i^{\uparrow}(\theta)}}{\boxed{\tau_i(\theta)}}$$

- **Atmospheric Parameters:** $\tau_i(\theta)$, $L_i^{\uparrow}(\theta)$, $L_i^{\downarrow}(\theta)$

  Estimated using radiative transfer code such as MODTRAN with Atmospheric profiles and elevation data

- Derivation of e_i and T_s is an undetermined problem

  The number of parameters (T_s, e_i in N channels) is always greater than the number of simultaneous equations needed to solve the problem (N)

  =>Additional, independent constraint is needed

Temperature/Emissivity Separation (TES)

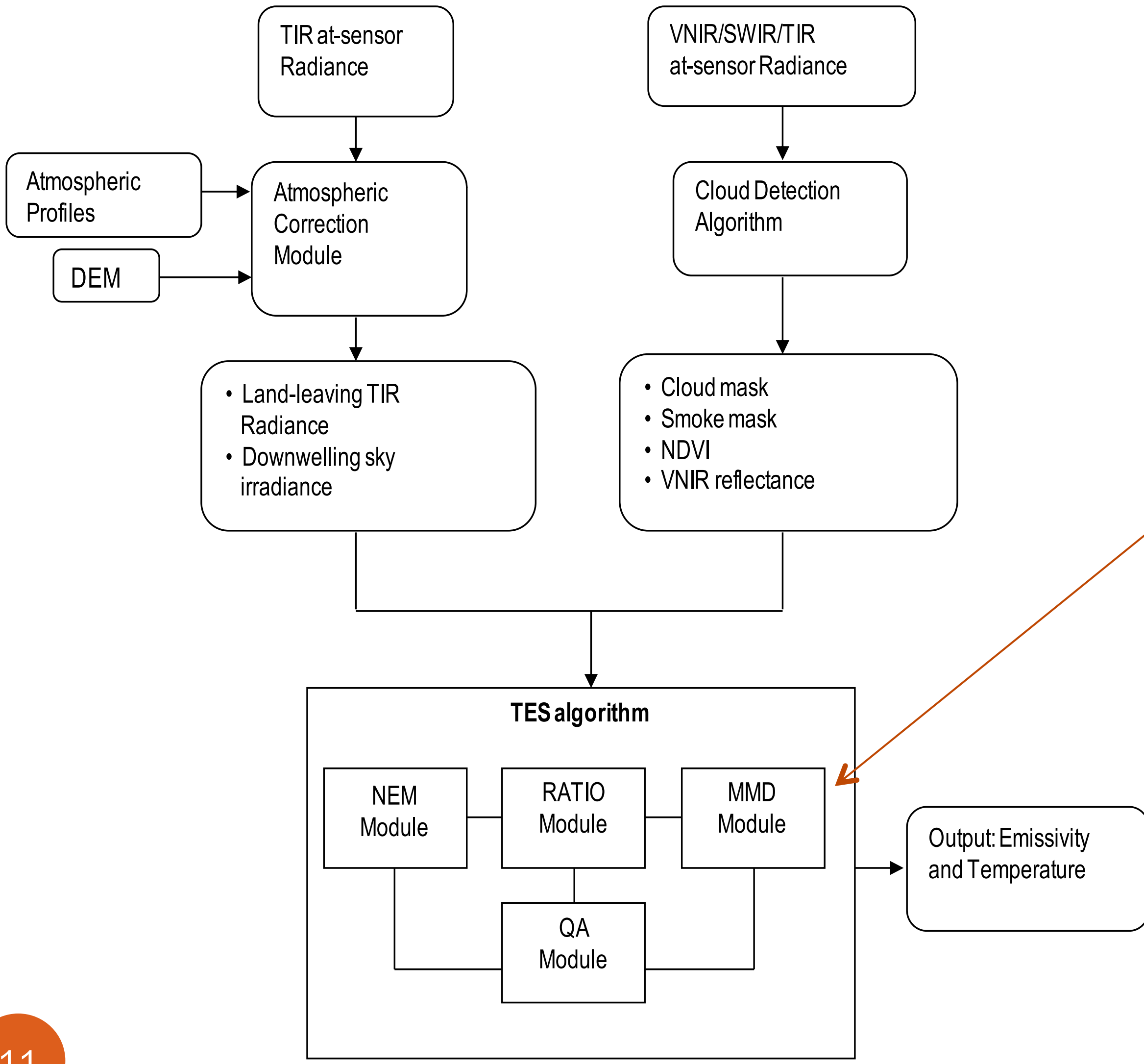

Calibration Curve

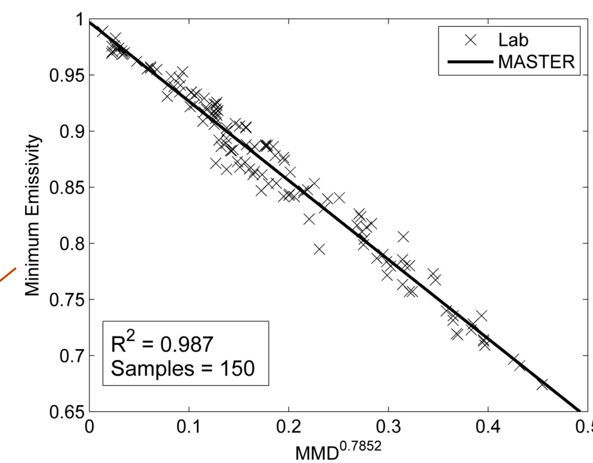

ASTER & MODIS Emissivity spectra for the Salton Sea showing effects of water vapor scaling (wvs)

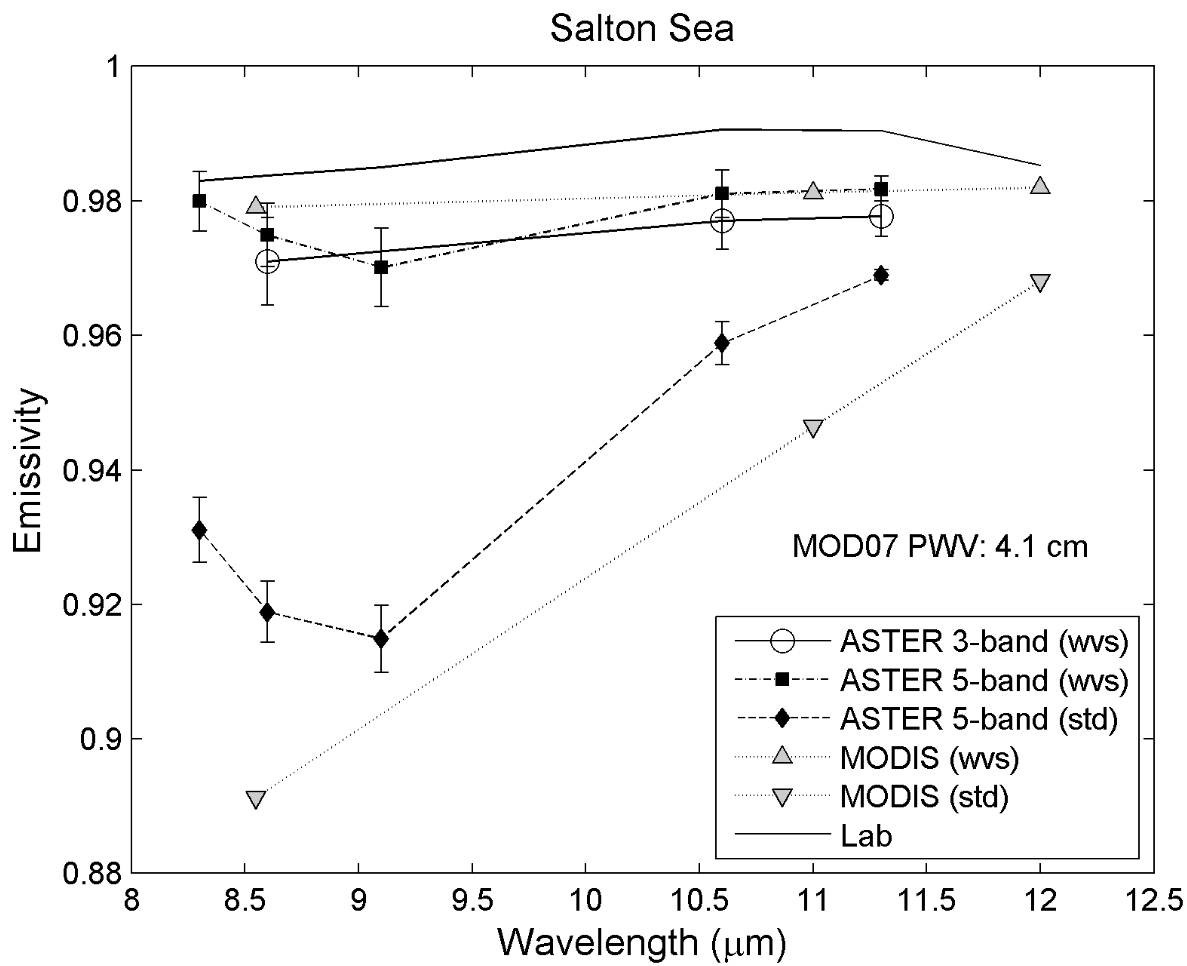

Now lets look at some products!

ASTER band 12 Emissivity

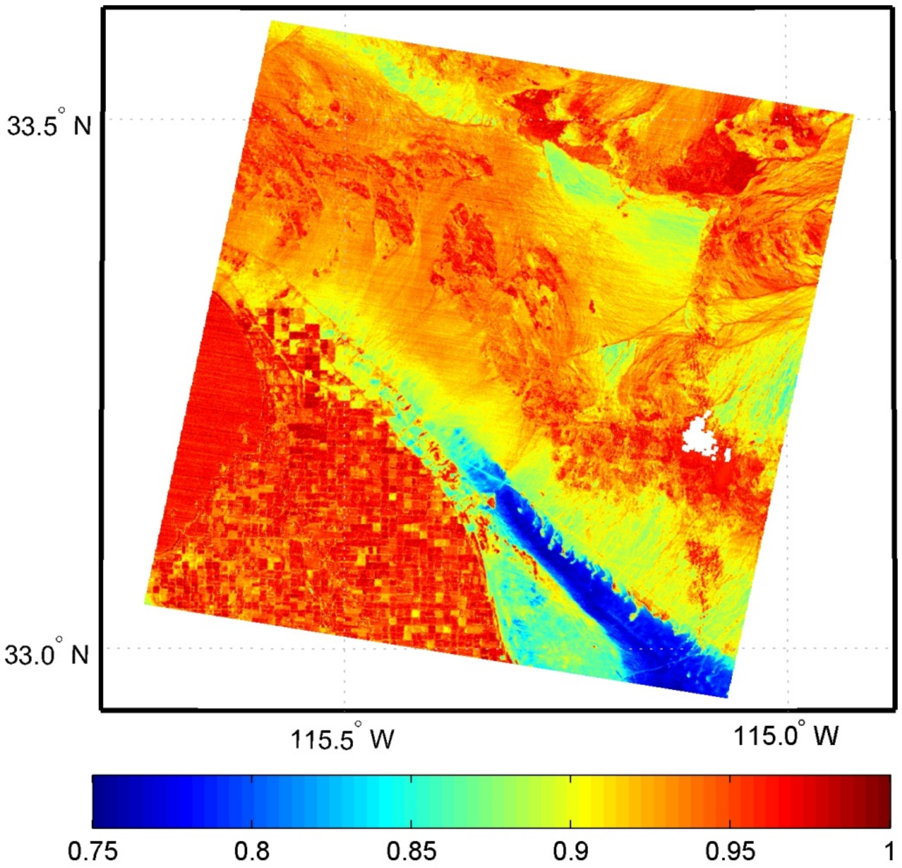

ASTER Land Surface Temperature (K)

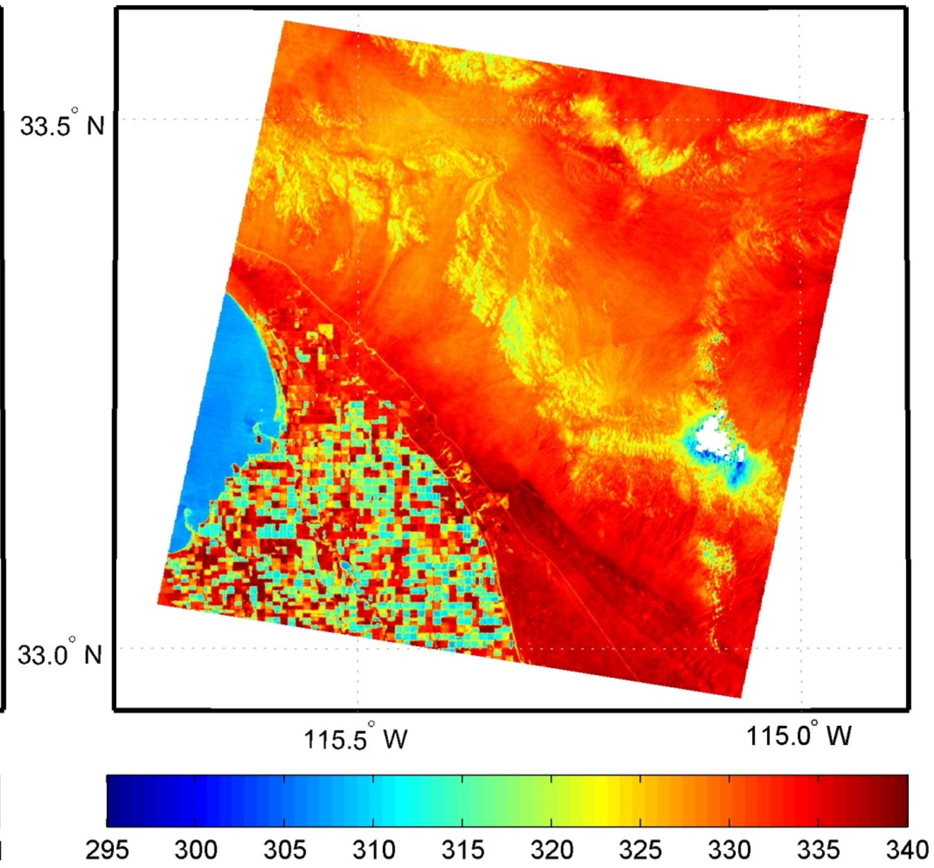

The ASTER Global Emissivity Map (GEM)

- ASTER produces Level-2 LST&E products at 90m
- Scenes (60 x 60 km) produced on demand, limited repeat (16 days) with no L-3 gridded data
- ASTER-GEM: Long-term mean gridded composite of all ASTER scenes acquired since 2000 at 100m, 1km, 5km, 50km resolution
  - Summertime (Jul-Sep), 2000-present
  - Wintertime (Jan-Mar), 2000-present
- Progress:
  - North America (JPL)
  - Africa & Arabian Peninsula (JPL, Tonooka)
  - Australia (JPL)
  - Asia and Europe (Tonooka)

NAALSED Summertime Emissivity (Jul-Sep 2000-2010), Band 12 (9.1 μm), 5km

Lowest emissivity over southwest

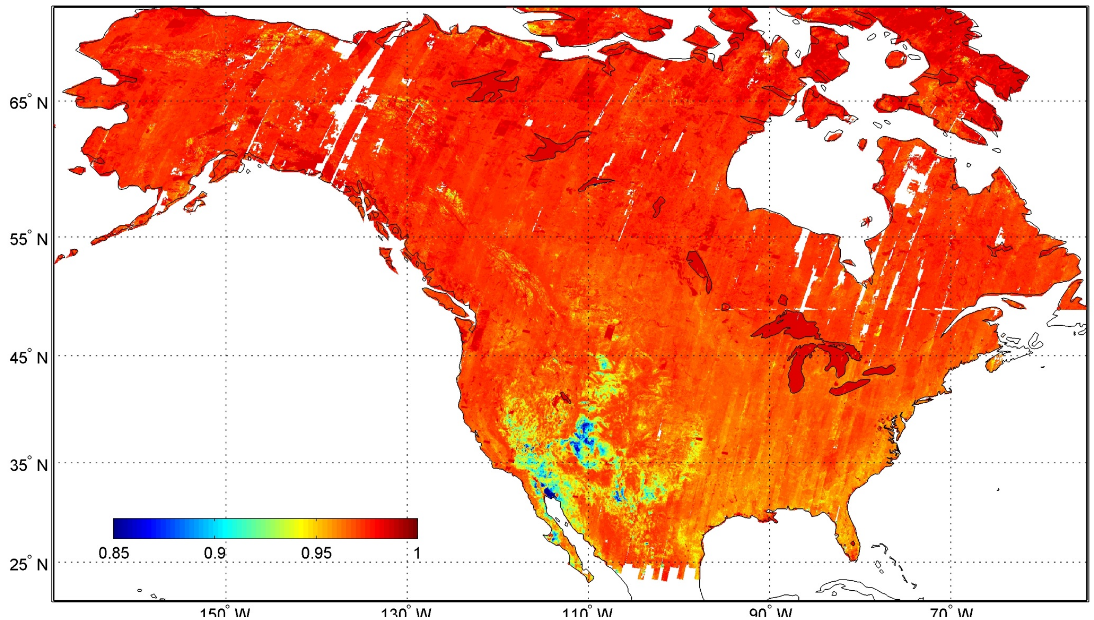

Number of pixels averaged for a given location ->

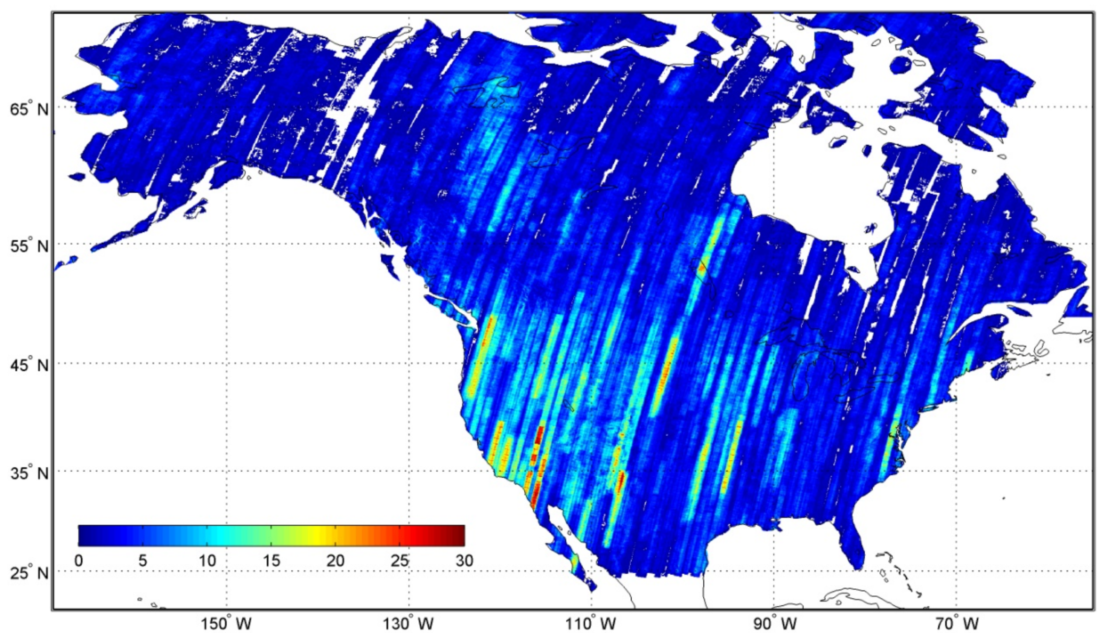

ASTER-GEM Band 12 emissivity (9.1 µm)
5km resolution: 2000-2010 (~112,000 scenes)

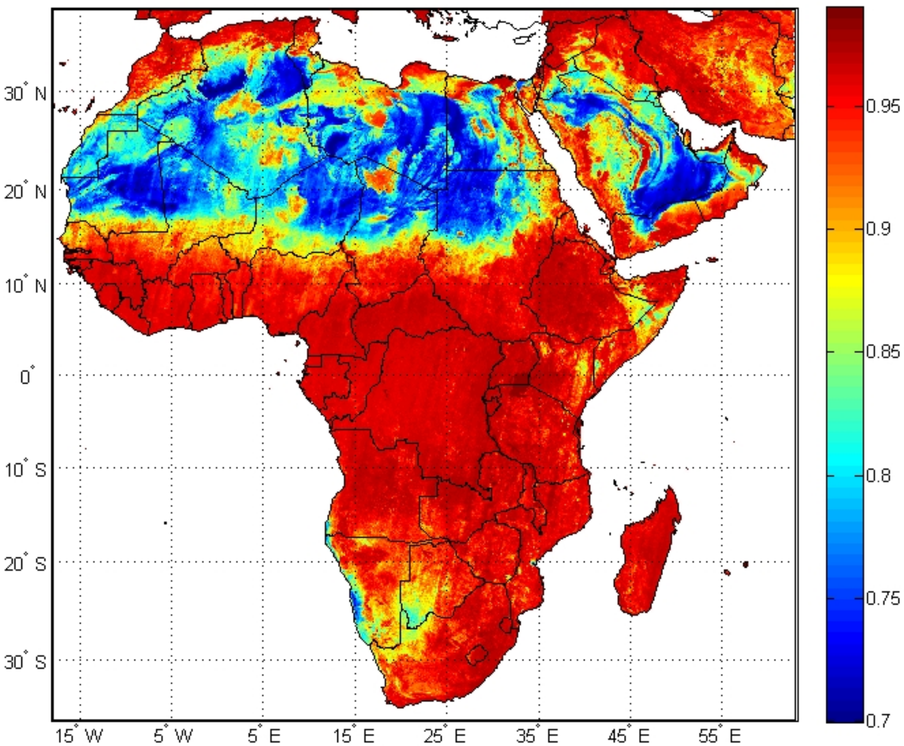

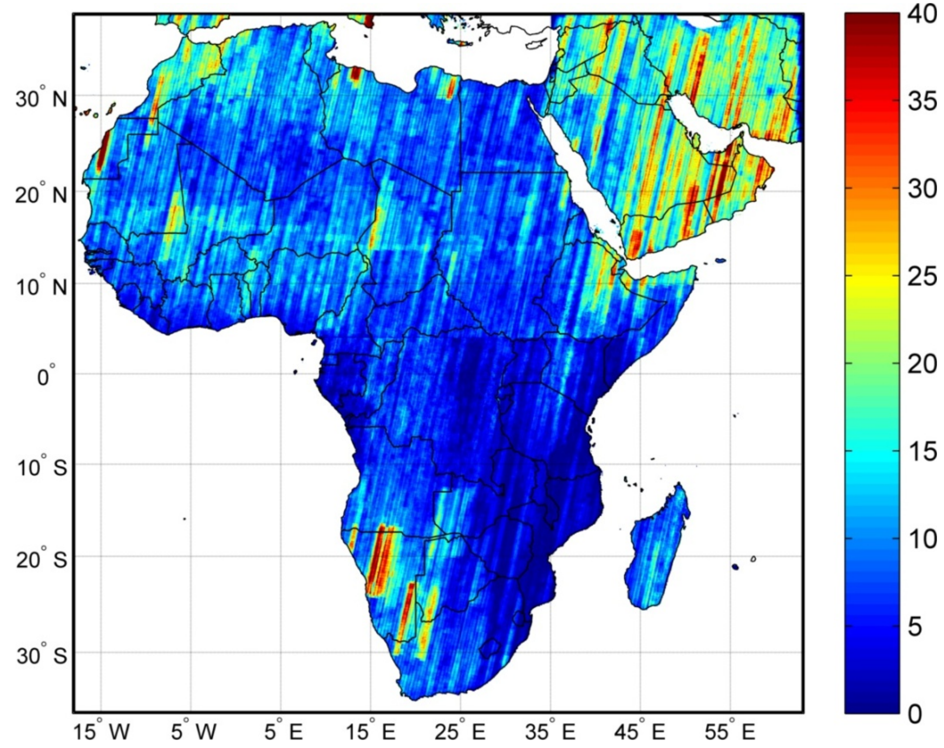

Certain regions have far more coverage than others!

ASTER-GEM Band 12 emissivity (9.1 μm)
5km resolution: 2000-2010

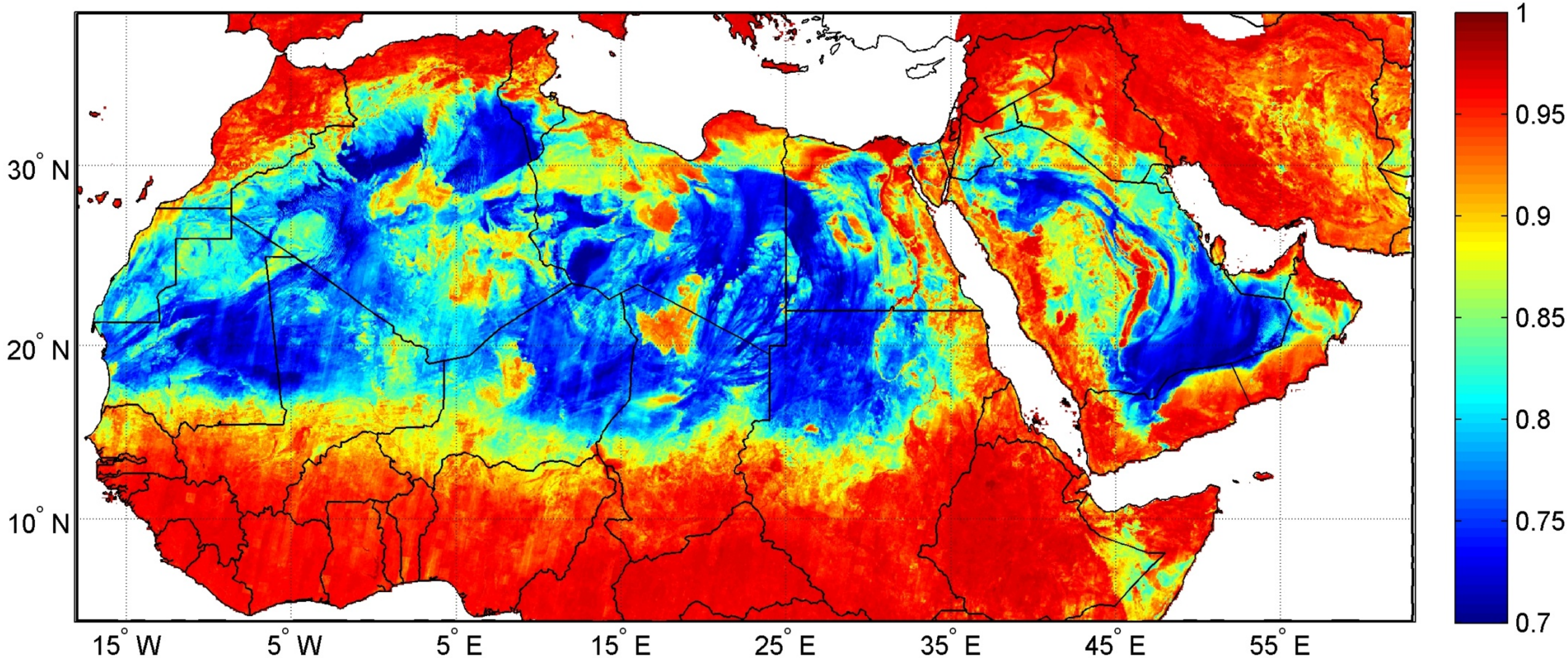

At 100 m spatial resolution see tremendous variation in emissivity (see next slide from Nambia)

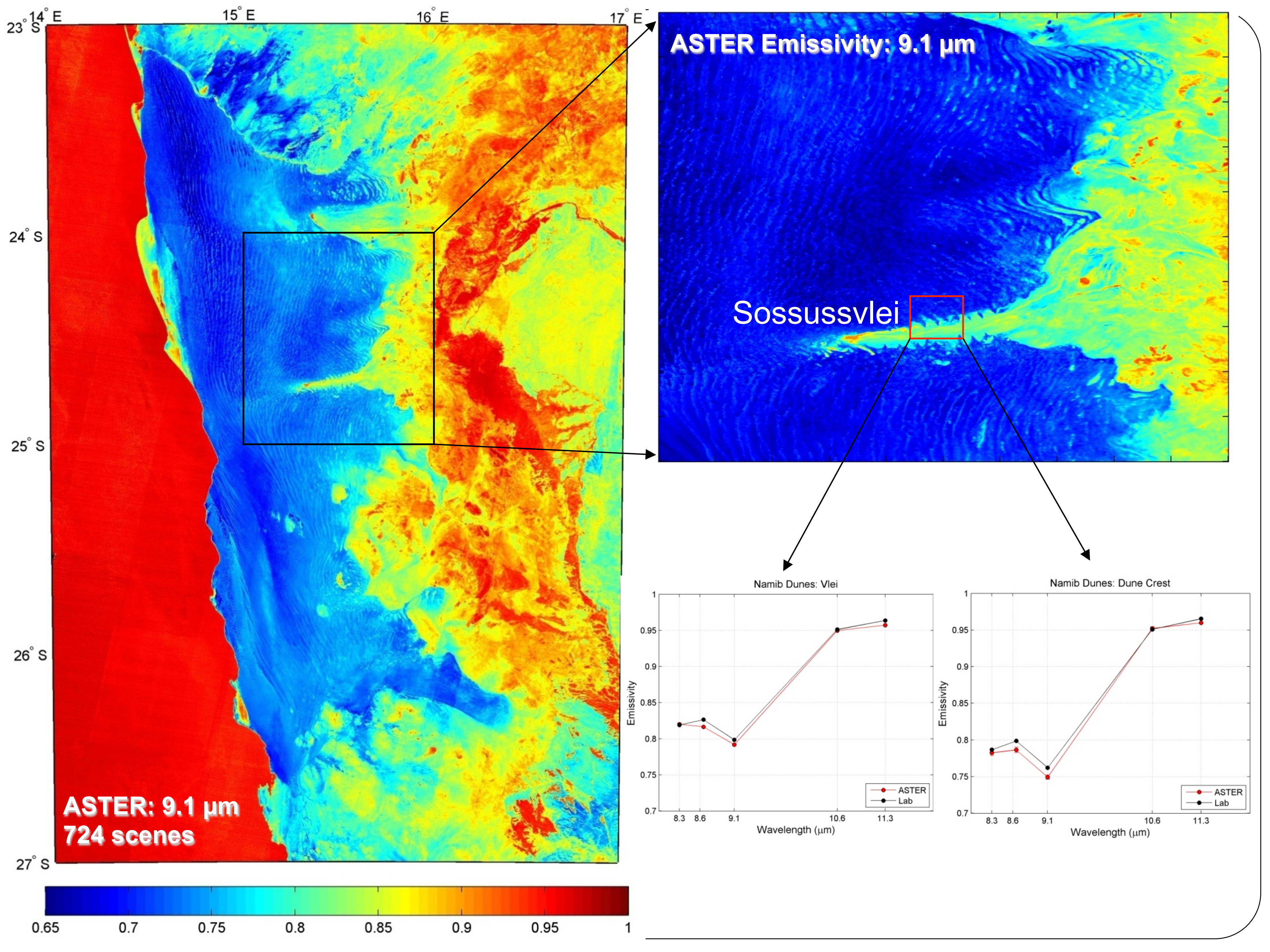

14° E
15° E
16° E
17° E
23° S
24° S
25° S
26° S
27° S
ASTER: 9.1 µm
724 scenes
0.65
0.7
0.75
0.8
0.85
0.9
0.95
1
ASTER Emissivity: 9.1 µm
Sossussvlei
Namib Dunes: Vlei
Namib Dunes: Dune Crest
Emissivity
Wavelength (µm)
8.3
8.6
9.1
10.6
11.3
ASTER
Lab

ASTER Global Emissivity Map (GEM): Death Valley

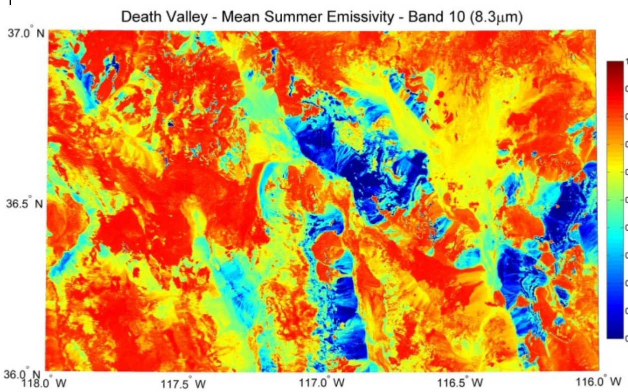

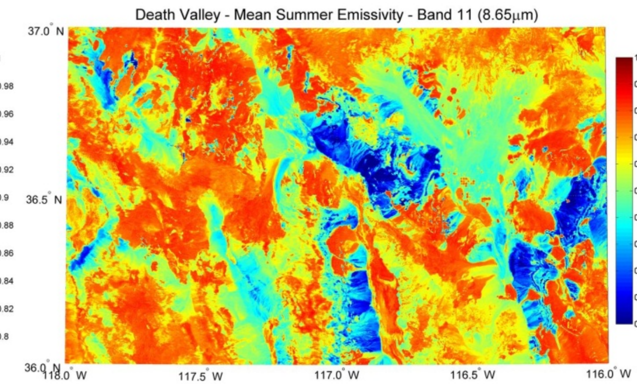

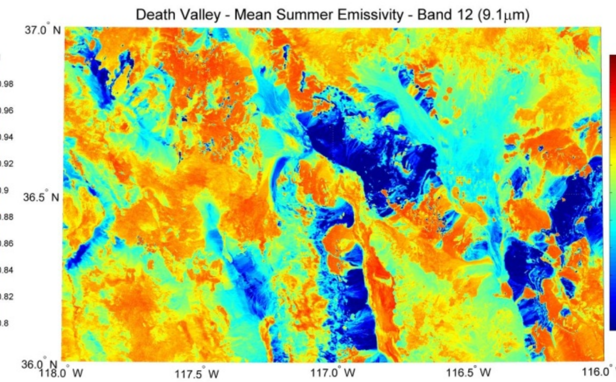

With HyspIRI we will produce similar products!

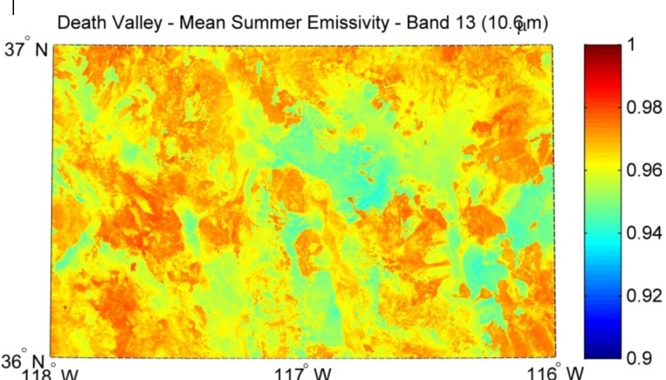

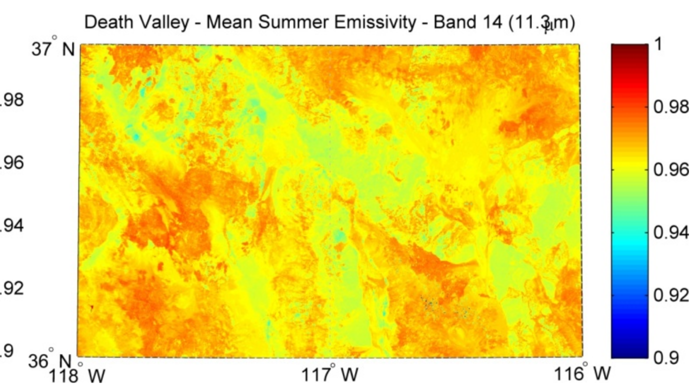

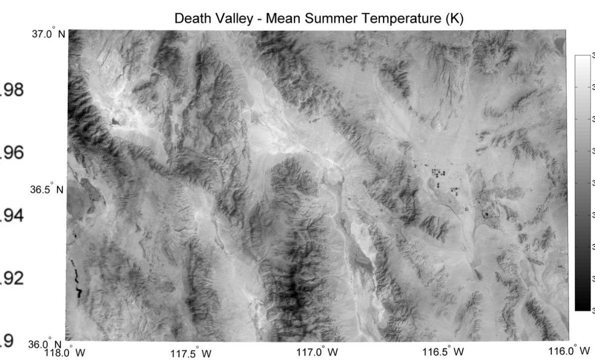

Less variation at longer wavelengths, hence the use of long wave IR Bands in split-window algorithms

Death Valley - Decorrelation Stretch - RGB (Band 14,12,10)

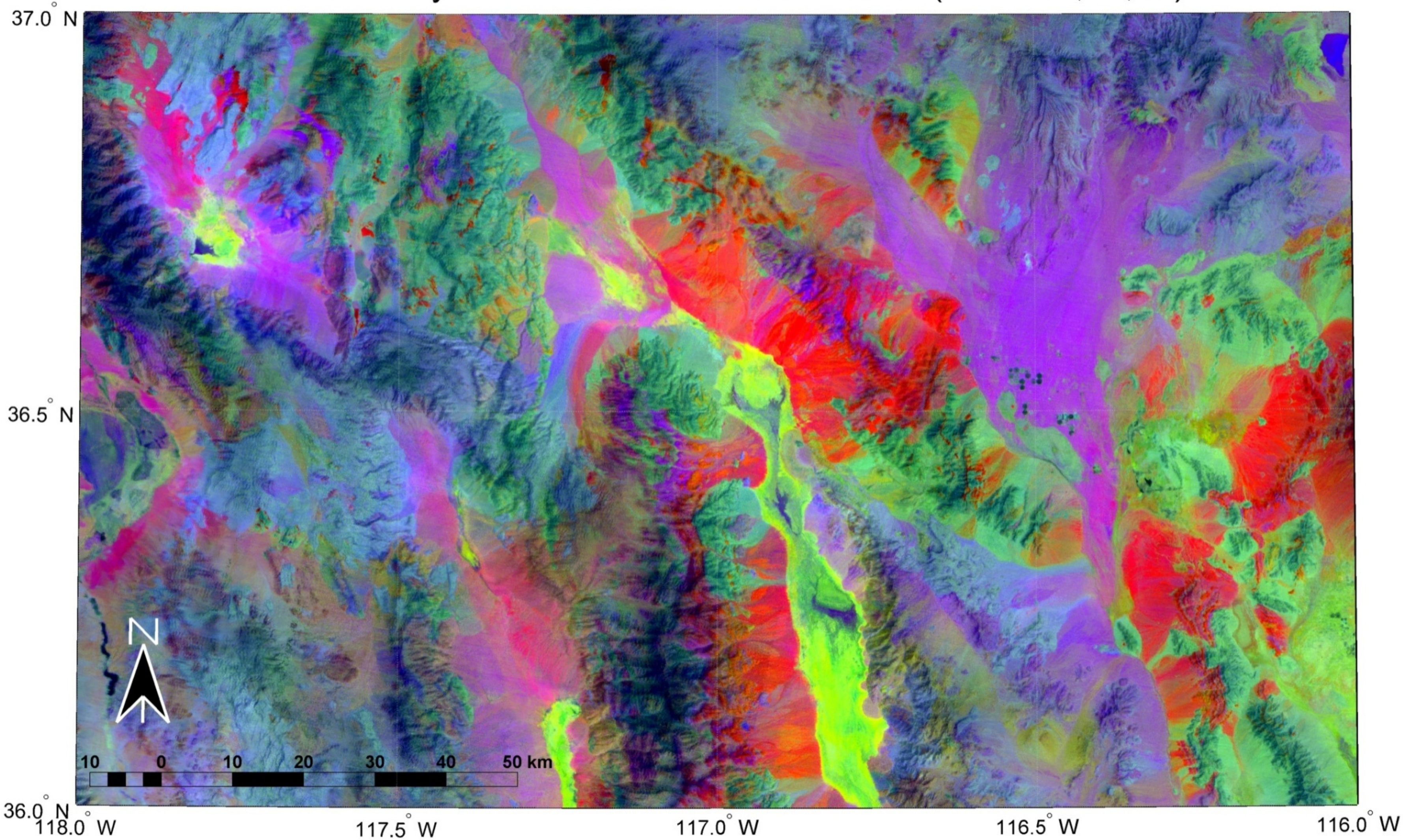

- Quartz-rich
- Carbonates
- Quartz-poor

Can use average temperature and emissivites to reconstruct a destretch without noise!

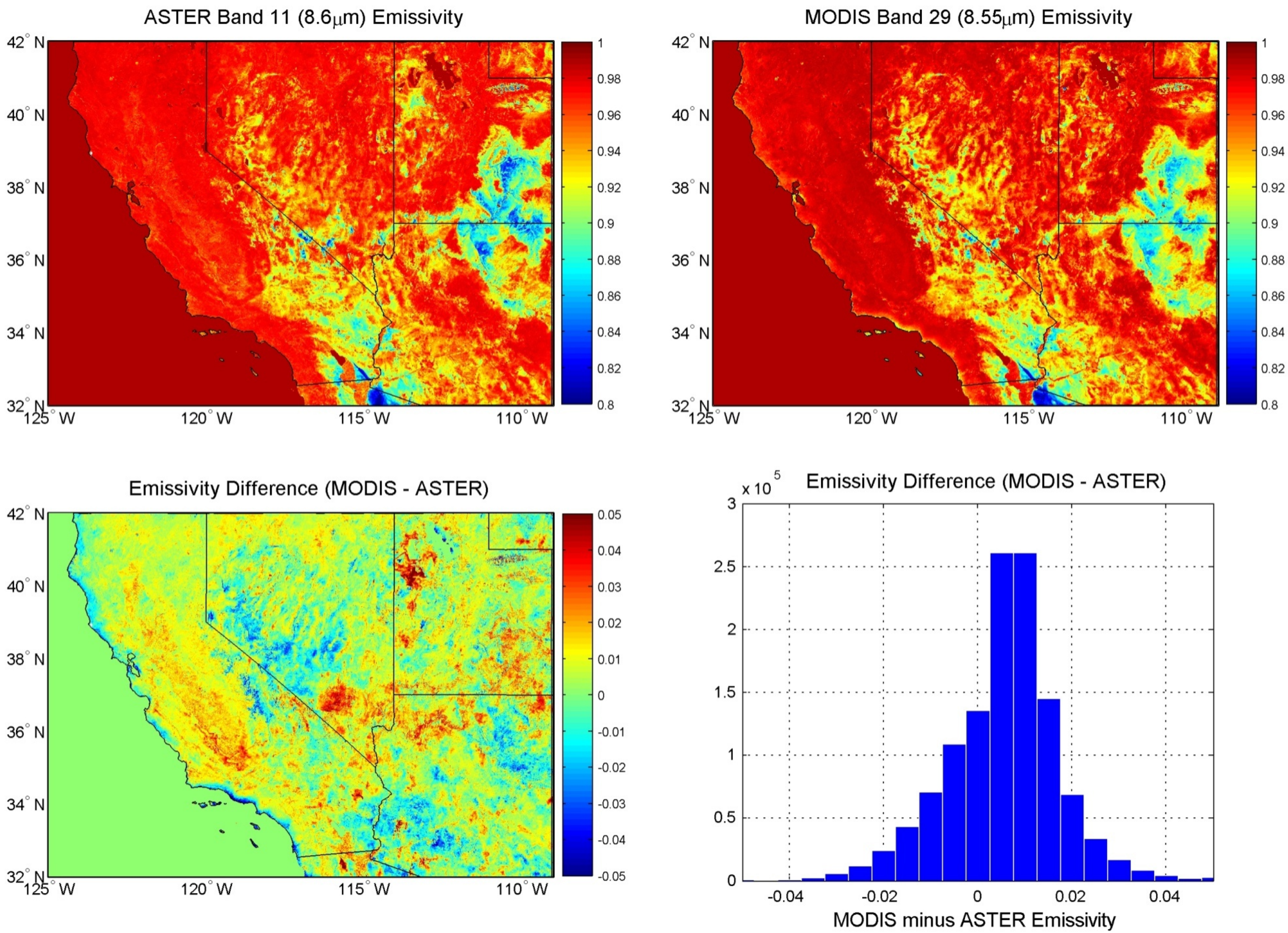

MOD21 product uses same algorithm as ASTER and provides 1km resolution emissivity

MODIS Temperature Emissivity Separation (MODTES) – MOD21_L2

- A new MODIS LST&E Product
- Generated using the ASTER Temperature/Emissivity Separation (TES) Algorithm with WVS
- Output: LST and emissivity for MODIS bands 29, 31, 32 at 1km spatial resolution
- Currently undergoing testing at MODAPS
- Future work:
  - Product testing and inter-comparisons
  - Validation (Radiance-based, Temperature-based)
  - Product ATBD

MOD21 Land Surface Temperature [K], 8-day mean, August 2004

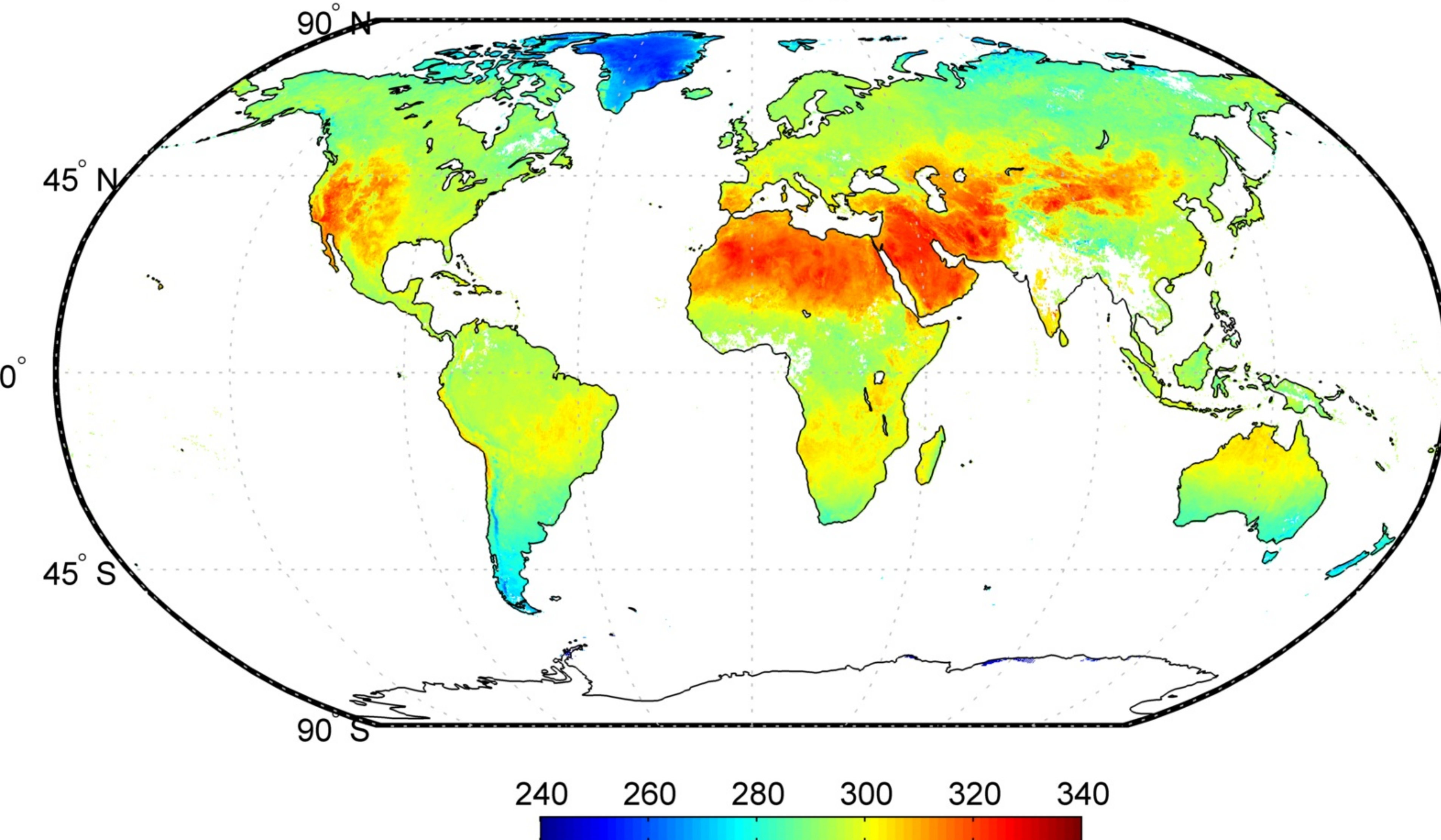

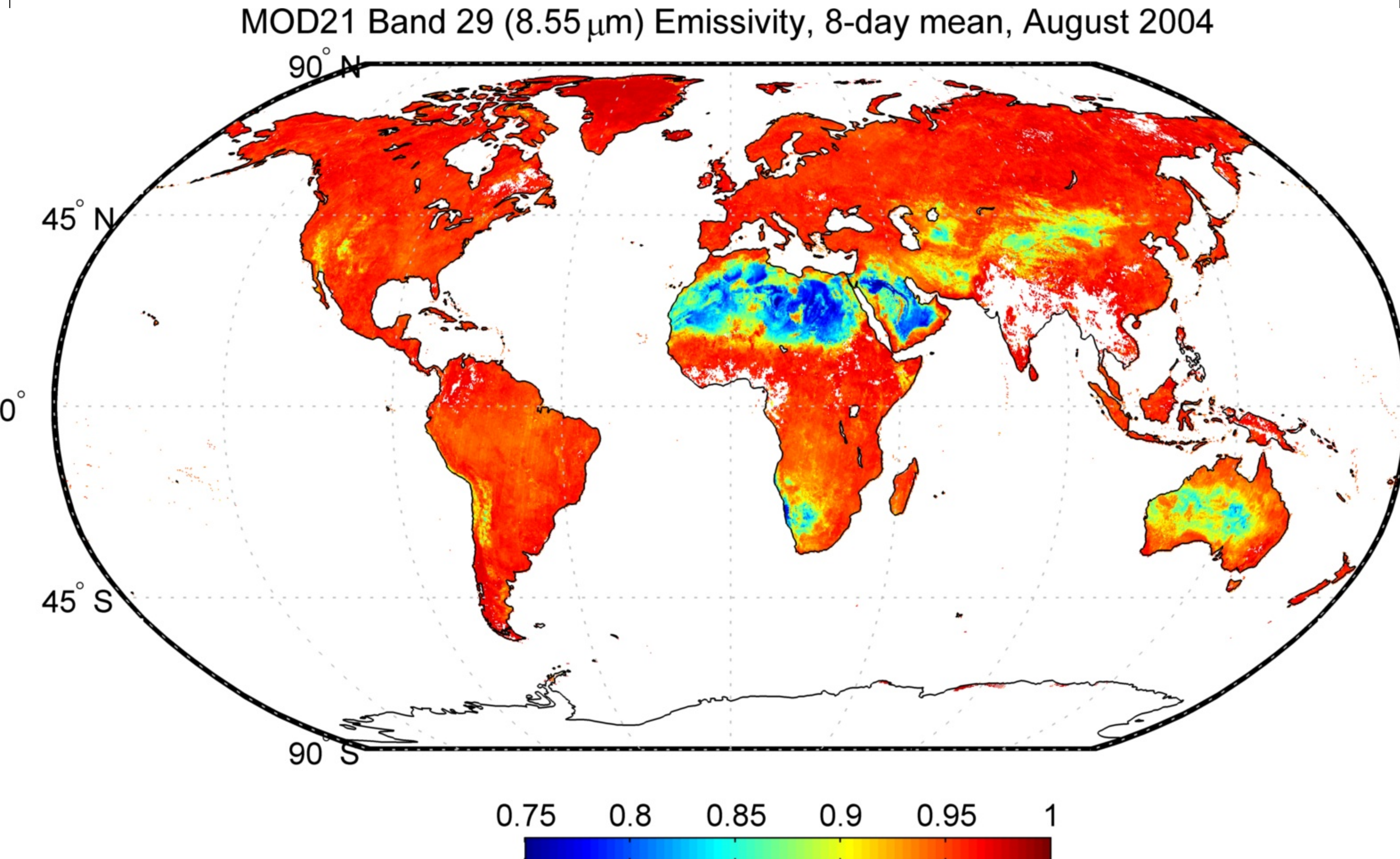

Great variation globally associated with reststrahlen band (Si-O stretching region)

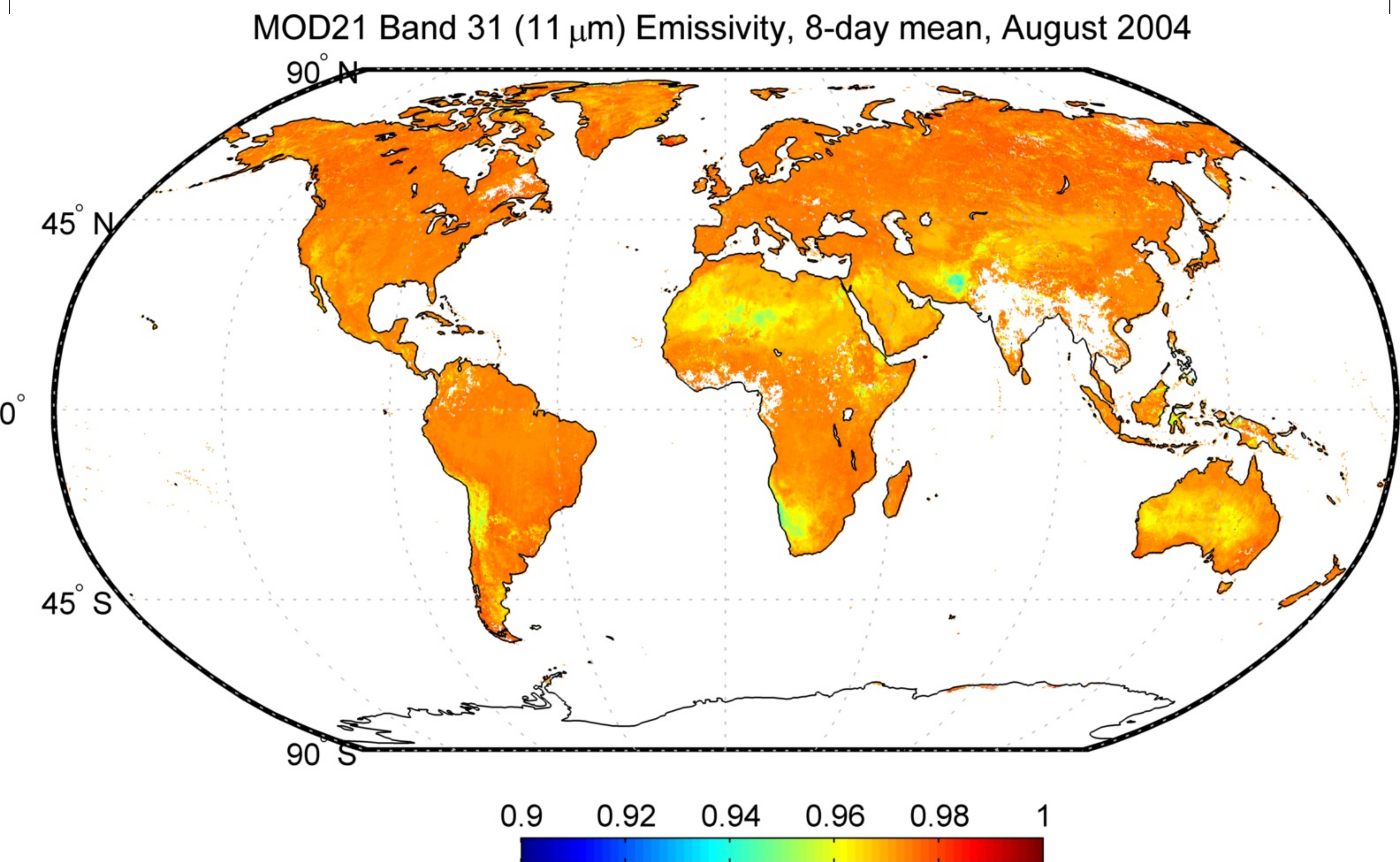

MOD21 Band 31 (11 μm) Emissivity, 8-day mean, August 2004
90° N
45° N
0°
45° S
90° S
0.9
0.92
0.94
0.96
0.98
1

MOD21 Band 32 (12 μm) Emissivity, 8-day mean, August 2004

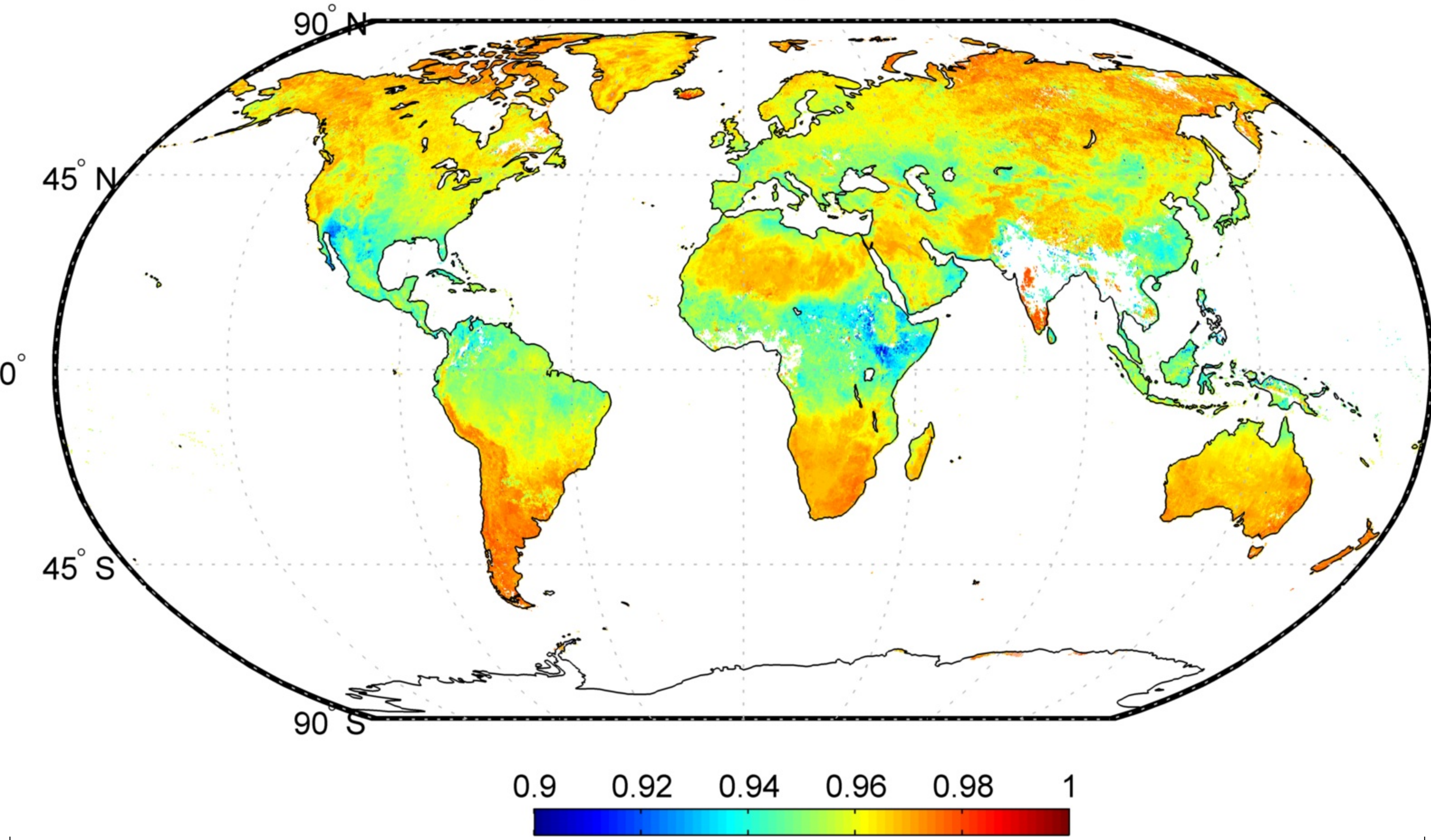

Variation in Band 32 highlights problems with split window algorithms which assume emissivity is constant

Emissivity Validation: Pseudo-Invariant sand dune sites

- Emissivity is notoriously difficult to validate. Typically large homogeneous areas with known composition are required (possible with ASTER – 90m)
- Large Sand-dune sites consistent mineralogy and physical properties over long time periods
- Rapid infiltration after rains, and drying of surface does not lead to cracks
- Mineralogy and composition can be accurately determined using lab reflectance and X-ray diffraction measurements at JPL
- **Sand-dune validation sites:**

Algodones dunes, El Centro, California

White Sands National Monument, New Mexico

Stovepipe Wells Dunes, Death Valley, California

Kelso Dunes, Mojave Desert, California

Great Sands National Park, Colorado

Sand Hollow State Park, Utah

Coral Pink Sand Dunes, Utah

Little Sahara, Utah

Killpecker Dunes, Wyoming

Moses Lake, Washington

ALGODONES DUNES, California

Sand Dune Validation Results

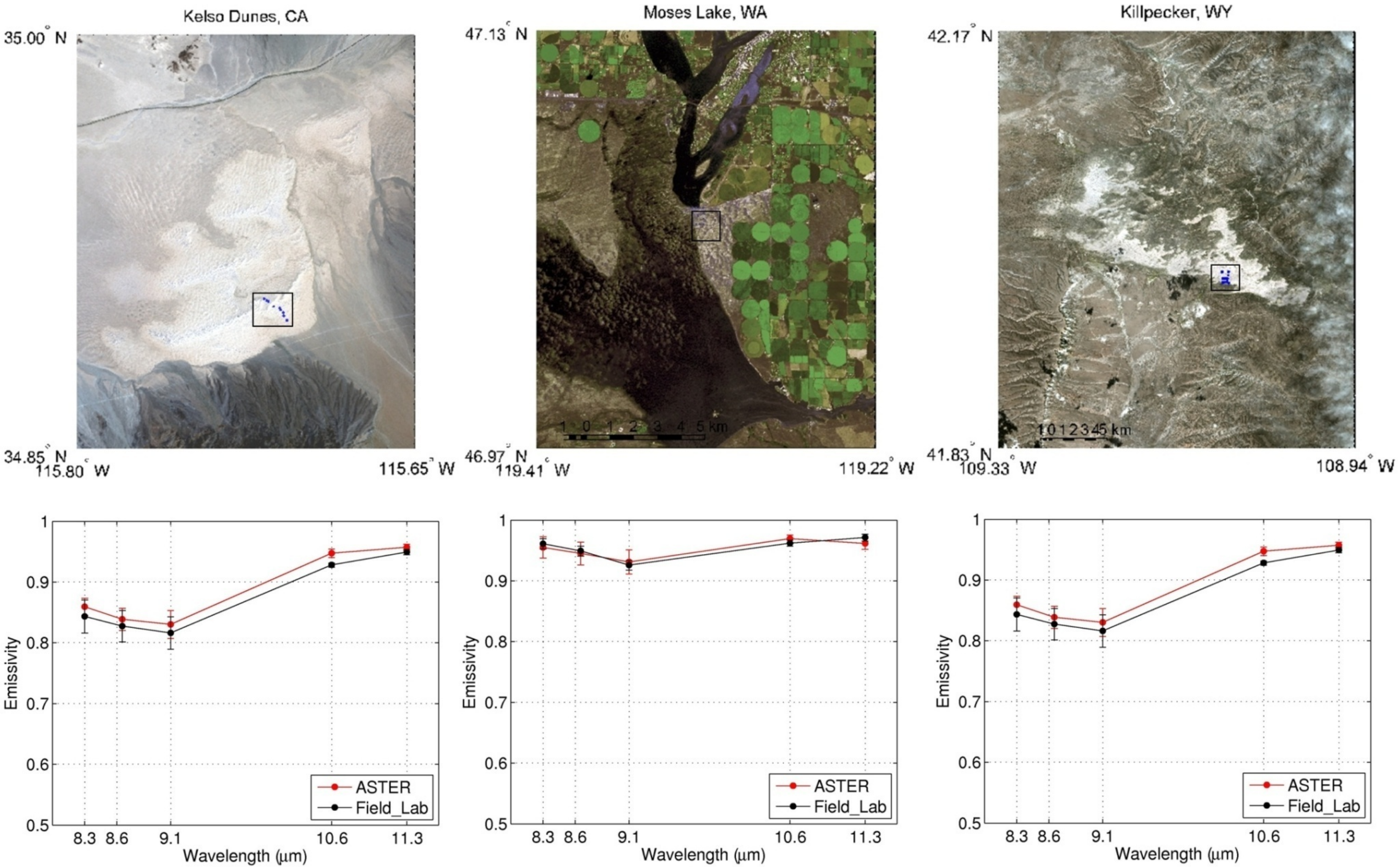

Hulley, G. C., Hook, S. J., and A.M. Baldridge, Validation of the North American ASTER Land Surface Emissivity Database (NAALSED) Version 2.0, *Remote Sensing of Environment* (2009), accepted

Sand Dune Emissivity Validation Results

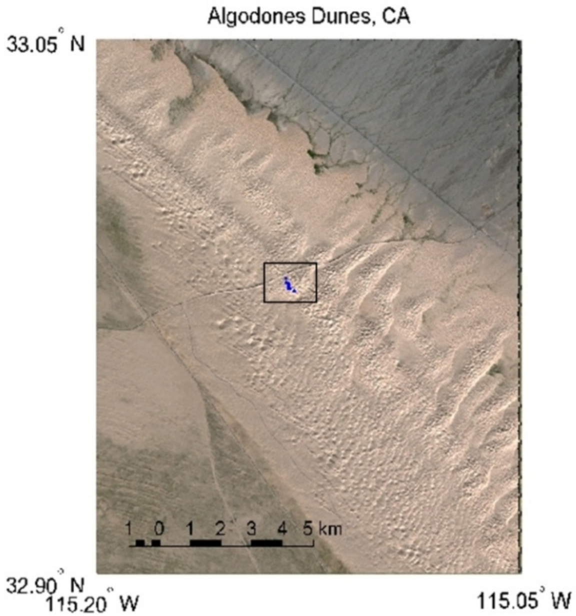

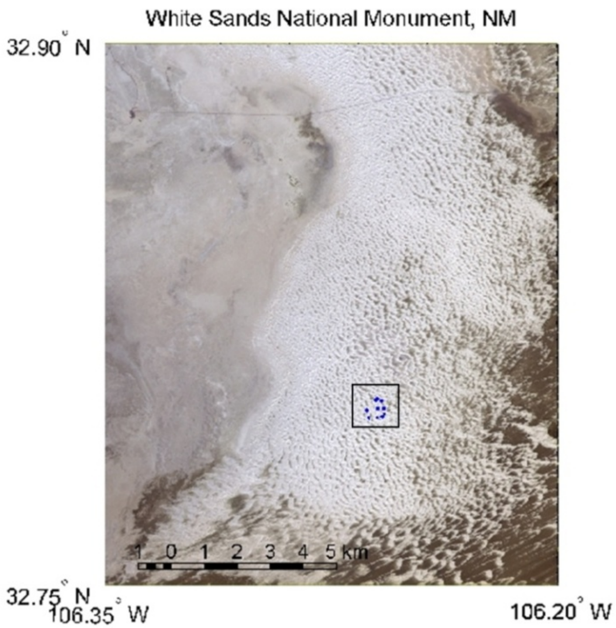

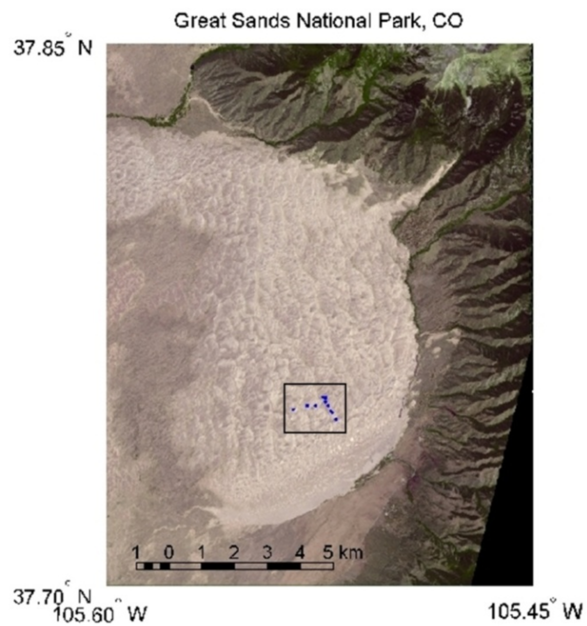

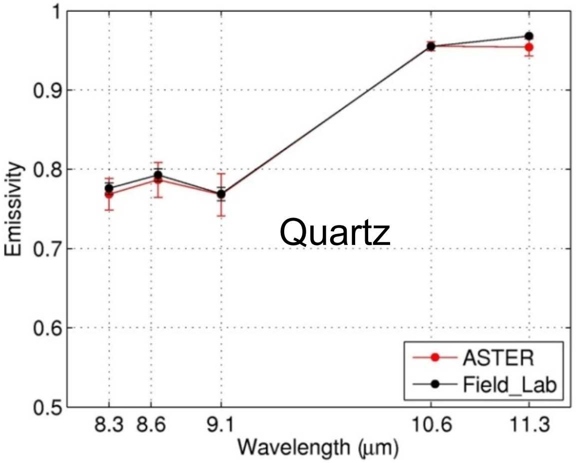

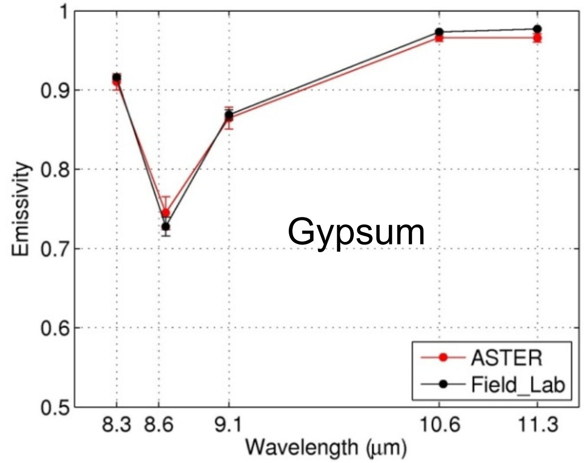

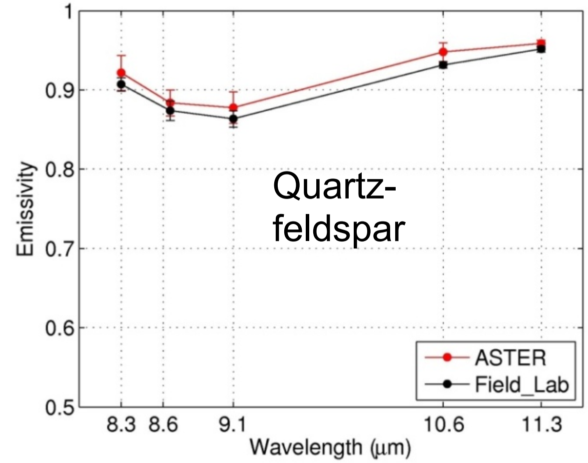

Hulley, G. C., Hook, S. J., and A.M. Baldridge, Validation of the North American ASTER Land Surface Emissivity Database (NAALSED) Version 2.0, *Remote Sensing of Environment* (2009), accepted

The End

National Aeronautics and Space Administration

Jet Propulsion Laboratory
California Institute of Technology
Pasadena, California

www.nasa.gov

JPL 400-1278 7/06

WVS Scaling Factor, γ

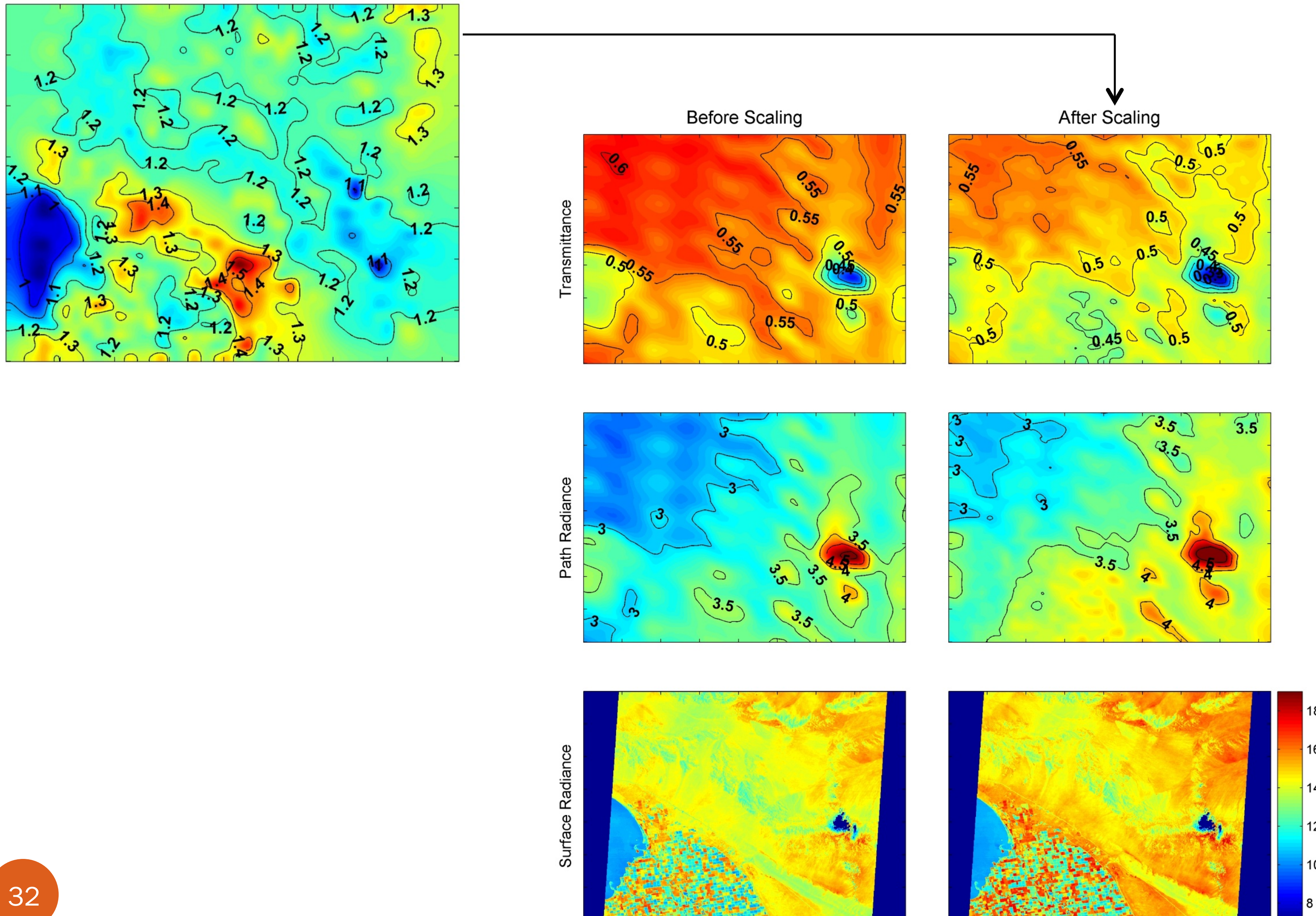


GREAT SANDS, Colorado
24 June, 2008
104 km²
Major: Quartz
Minor: Feldspar


WHITE SANDS, New Mexico
20 May, 2008
704 km²
Major: Gypsum

Sand samples collected in field

Reflectance measured using Nicolet 520 FTIR spectrometer

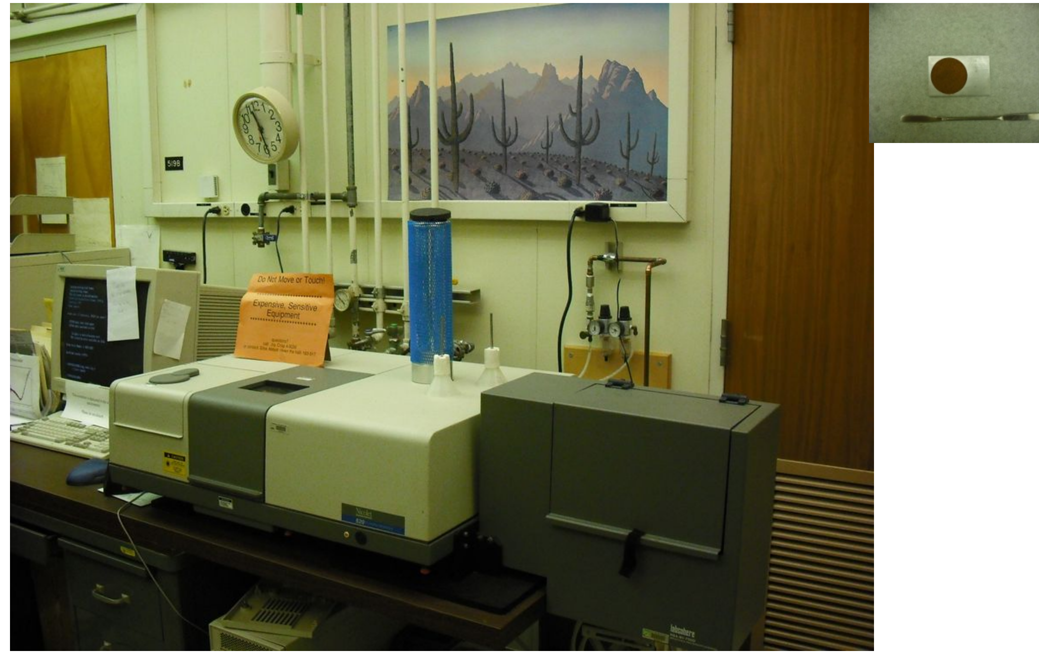

JPL

LAB MEASUREMENTS

$\varepsilon = 1 - r$

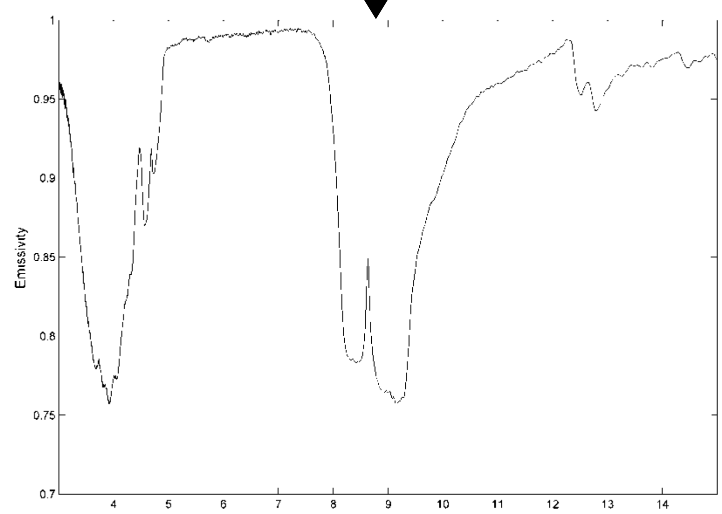

spectral range: 2.5 – 15 μm

spectral resolution: 4 cm^{-1}

1000 scans in 10 minutes

Pseudo-Invariant Sand Dune Sites

Table 1
Summary of the major characteristics of each dune site including locality, elevation, surface area, dune height, grain size, sand source and bulk mineralogy.

Dune site	Locality	Surface area (km^2)	Elevation/max dune height (m)	Grain size	Sand source	Mineralogy (XRD)
Algodones (32.95° N, 115.07° W)	Southeast CA, Eastern margin of the Salton Trough	720	94/80	Medium to coarse sand	Beach sand from Lake Cahuilla	Major: quartz
Coral Pink (37.04° N, 112.72° W)	Sand Valley, just north of UT–AZ border, west Kanab	13.6	1780/10	Medium sand	Navajo, Page and Estrada Jurassic sandstones of the Vermillion Cliffs	Major: quartz
Great Sands (37.77° N, 105.54° W)	San Luis Valley, CO, adjacent to Sangre de Cristo, NE of Alamosa	104	2560/230	Medium to coarse sand	Quartz and volcanic fragments derived from Santa Fe and Alamosa formations, recent fluvial (Rio Grande) deposits	Major: quartz Minor: potassium feldspar
Kelso (34.91° N 115.73° W)	Mojave Desert, CA, southeast of Baker	115	800/195	Medium sand	Derived from sedimentary, metamorphic, igneous terrains from Mojave River alluvial apron	Major: quartz Minor: potassium feldspar Trace: magnetite
Killpecker (41.98° N 109.10° W)	Southwest WY, from Eden across Rock Springs into Red Desert	550	2000/45	Medium sand	Sandstone and siltstone of the Laney member of the Green River Formation	Major: quartz Trace: magnetite Minor: plagioclase feldspar, epidote
Little Sahara/Lynndyl (39.7° N 112.39° W)	West-central UT, Sevier River drainage basin, west of Lynndyl	575	1560/200	Fine sand	Deltaic and shoreline sediments from the Provo shoreline of Lake Bonneville	Major: quartz Minor: plagioclase feldspar, pyroxene, carbonate, magnetite
Stovepipe Wells (36.62° N, 117.11° W)	Central Death Valley, CA, near Stovepipe Wells	7.7	−12/40	Medium sand	Mixed lithic fragments and quartz from Emigrant Pass to the west and Furnace Wash to the east	Major: quartz Minor: plagioclase feldspar, potassium feldspar
Moses Lake (47.05° N, 119.31° W)	Quincy Basin in central WA	40	345/18	Fine sand	Basaltic sand from the east bank of the Columbia River	Major: quartz, albite
White Sands (32.89° N, 106.33° W)	South-central NM, Tularosa Valley	704	1216/10	Fine sand	Paleo-lake Otero, present playa Lake Lucero to the southwest	Major: gypsum

Hulley, G. C., Hook, S. J., and A.M. Baldridge, (2009), Validation of the North American ASTER Land Surface Emissivity Database (NAALSED) Version 2.0, *Remote Sensing of Environment*, 113, 2224-2233

ASTER validation with pseudo-invariant sand dune sites

	ASTER MINUS LAB EMISSIVITY (%)					
Dune site	**Band 10**	**Band 11**	**Band 12**	**Band 13**	**Band 14**	**Mean**
Algodones	0.68	0.60	0.13	0.02	1.40	**0.57**
Stovepipe Wells	0.17	0.77	1.02	0.34	0.37	**0.53**
White Sands	0.34	2.76	0.16	0.92	1.08	**1.05**
Kelso Dunes	1.57	1.04	1.33	1.91	0.81	**1.33**
Great Sands	1.44	0.97	1.42	1.64	0.69	**1.23**
Moses Lake	0.69	0.52	0.42	0.61	1.01	**0.65**
~~Sand Mountain~~	~~7.74~~	~~6.47~~	~~9.01~~	~~1.82~~	~~1.10~~	~~**5.23**~~
Coral Pink	7.48	6.44	7.32	2.50	1.70	**4.90**
Little Sahara	3.55	2.39	2.60	0.96	0.19	**1.94**
Killpecker	2.34	1.99	2.26	1.33	0.81	**1.75**

< 1.6% (1 K)